Acta Pharmaceutica Sinica B 2025;15(2):934–946

Chinese Pharmaceutical Association
Institute of Materia Medica, Chinese Academy of Medical Sciences

Acta Pharmaceutica Sinica B

www.elsevier.com/locate/apsb
www.sciencedirect.com

ORIGINAL ARTICLE

Protection efficacy of mRNA-based SARS-CoV-2 variant vaccine in non-human primates

Dongrong Yi[a,†], Yongxin Zhang[a,†], Jing Wang[a,†], Qian Liu[b,†], Ling Ma[a,†], Quanjie Li[a,†], Saisai Guo[a], Ruifang Zheng[c], Xiaoyu Li[a], Xingong Li[d], Yijie Dong[d], Shuaiyao Lu[e,*], Weiguo Zhang[d,*], Xiaozhong Peng[b,e,f,*], Shan Cen[a,*]

[a]*Institute of Medicinal Biotechnology, Chinese Academy of Medical Sciences, Beijing 100050, China*
[b]*Institute of Basic Medical Sciences, Chinese Academy of Medical Sciences, Beijing 100005, China*
[c]*Xinjiang Key Laboratory of Uygur Medical Research, Xinjiang Institute of Materia Medica, Urumqi 830004, China*
[d]*RinuaGene Biotechnology Co., Ltd., Suzhou 215127, China*
[e]*Institute of Medical Biology, Chinese Academy of Medical Sciences, Kunming 650118, China*
[f]*Institute of Laboratory Animals Science, Chinese Academy of Medical Sciences, Beijing 100021, China*

Received 6 June 2024; received in revised form 21 July 2024; accepted 26 July 2024

KEY WORDS

SARS-CoV-2;
mRNA-LNP;
Vaccine;
Spike glycoprotein;
Non-human primate;
Humoral immunity;
Cellular immunity;
Circulating Omicron sublineages

Abstract The rapid emergence of severe acute respiratory syndrome coronavirus 2 (SARS-CoV-2) variants that evade immunity elicited by vaccination has posed a global challenge to the control of the coronavirus disease 2019 (COVID-19) pandemic. Therefore, developing countermeasures that broadly protect against SARS-CoV-2 and related sarbecoviruses is essential. Herein, we have developed a lipid nanoparticle (LNP)-encapsulated mRNA (mRNA-LNP) encoding the full-length Spike (S) glycoprotein of SARS-CoV-2 (termed RG001), which confers complete protection in a non-human primate model. Intramuscular immunization of two doses of RG001 in Rhesus monkey elicited robust neutralizing antibodies and cellular response against SARS-CoV-2 variants, resulting in significantly protected SARS-CoV-2-infected animals from acute lung lesions and complete inhibition of viral replication in all animals immunized with low or high doses of RG001. More importantly, the third dose of RG001 vaccination elicited effective neutralizing antibodies against current epidemic XBB and JN.1 strains and

*Corresponding authors.
E-mail addresses: shancen@imb.pumc.edu.cn (Shan Cen), pengxiaozhong@pumc.edu.cn (Xiaozhong Peng), weiguo.zhang@rinuagene.com (Weiguo Zhang), lushuaiyao-km@163.com (Shuaiyao Lu).
[†]These authors made equal contributions to this work.
Peer review under the responsibility of Chinese Pharmaceutical Association and Institute of Materia Medica, Chinese Academy of Medical Sciences.

https://doi.org/10.1016/j.apsb.2024.12.003

similar cellular response against SARS-CoV-2 Omicron variants (BA.1, XBB.1.16, and JN.1) were observed in immunized mice. All these results together strongly support the great potential of RG001 in preventing the infection of SARS-CoV-2 variants of concern (VOCs).

1. Introduction

In 2020, the World Health Organization (WHO) announced the global outbreak of SARS-CoV-2. The emergence of several VOCs, including Alpha, Beta, Gamma, Delta, and Omicron, led to five or six pandemic waves in many countries[1]. In particular, over 30 mutations have accumulated in Omicron S glycoprotein. These key amino acid changes are associated with the evasion of immune defense established by vaccine immunization[2,3] and breakthrough infections[4-6]. In the context of expanding population immunity, successive SARS-CoV-2 lineages have shown increasing capacity to evade both vaccine-derived and infection-derived immune responses throughout the COVID-19 pandemic. As the fifth VOC of SARS-CoV-2, the Omicron variant (B.1.1.529) has rapidly become the dominant type among the previous circulating variants worldwide. Recently, Omicron subvariants XBB and JN.1 have become global public health concerns due to their ability to evade therapeutic monoclonal antibodies and herd immunity induced by prior COVID-19 vaccines, boosters, and infections. Therefore, developing vaccines and therapeutics that are broadly effective against both known and emerging coronaviruses remains an urgent priority.

Among approved COVID-19 vaccines, mRNA-based vaccines were authorized for emergency use and exhibited excellent immunogenicity and protection[7]. Two approved mRNA vaccines, developed by Moderna (mRNA-1273) and Pifzer-BioNTech (BNT162b2), are based on the S protein of the ancestral SARS-CoV-2 strain. Immunization with these mRNA vaccines stimulated broad-spectrum neutralizing antibodies against various early VOCs, with favorable efficacy and safety[8-11]. Emerging SARS-CoV-2 mutant strains, particularly Omicron, continue to evolve to evade immune surveillance. To enhance vaccine-elicited neutralization against new SARS-CoV-2 VOCs, a third or fourth dose of BNT162b2 or mRNA-1273 has been shown to induce higher neutralizing antibody titers against B.1.1.529 (Omicron). However, their relatively weak neutralizing effects toward the Omicron sublineages are not sufficient to prevent symptomatic diseases[12-14]. Results from the pseudovirus neutralization assay showed that the newly emerged XBB subvariant is approximately 66- to 155-fold more resistant to neutralizing antibodies (nAbs) in the sera of vaccinated and infected individuals compared to the ancestral strain D614G[15]. Moreover, a bivalent booster vaccine expressing both BA.5 and ancestral S proteins has not generated sufficiently strong nAbs against XBB[16,17]. The neutralizing capacity of antibodies against XBB.1.5 and JN.1, elicited by three doses of BNT162b2 combined with a bivalent booster, was significantly reduced compared to D614G and Delta[18]. Moderna's mRNA-1273 series vaccine, mRNA-1273.529, developed using nucleotide sequence from the BA.1 S protein, was suggested as a booster immunization following primary vaccination with other vaccines. This booster could efficiently protect against BA.1 and BA.2 infections[19]. Omicron sublineages, particularly those that emerged after the BA.4/5 strain, evade nAb responses induced by BA.1 breakthrough infection. An updated XBB.1.5 monovalent mRNA vaccine has increased neutralizing antibody responses against the emerging Omicron subvariants, including JN.1[20]. However, Omicron S-based vaccines have failed to protect against earlier SARS-CoV-2 variants, such as Alpha and Delta[21,22]. Therefore, it is urgent to optimize vaccine immunogen design and formulations for SARS-CoV-2 variants[23]. This calls for the urgent need to develop a pan-sarbecovirus vaccine to combat all SARS-CoV-2 variants and subvariants.

In this work, we present a potential SARS-CoV-2 mRNA vaccine candidate, RG001, which encodes the full-length Delta variant S glycoprotein with several key amino acid changes that stabilize the pre-fusion conformation. This mRNA-LNP product has been manufactured under good manufacturing practice (GMP)-like conditions and can be easily scaled up upon demand. Evaluation in animal models, including mice and non-human primates vaccinated with RG001, indicated strong humoral and cellular immune responses and favorable host protection, comparable to approved mRNA vaccines. Notably, in addition to neutralizing historical SARS-CoV-2 VOCs, two to three doses of RG001 immunization provided strong protection against infection by circulating Omicron sublineages such as XBB.1.16 and JN.1. This might help partially address the urgent issue of Omicron breakthrough infection.

2. Materials and methods

2.1. Ethics statement

Mice protocols were approved by the Institutional Animal Care and Use Committee of the Institute of Laboratory Animal Science, Peking Union Medical College (BLL20001). Female BALB/c mice were purchased from Beijing Vital River Laboratory Animal Technology Co., Ltd. (SCXK(JING)2021-0006), and executed and housed in the Institute of Medicinal Biotechnology, Chinese Academy of Medical Sciences, Beijing, China. Nonhuman primate studies were performed at Kunming Institute of Zoology (KIZ), Chinese Academy of Sciences, Kunming, China. Rhesus macaques (2−3 years old) were provided by Yunnan Ren Li Kun Yuan Co., Ltd. (SCXK(DIAN)K2019-0001). Macaque experiments were reviewed and approved by the Experimental Animal Ethics Committee of the Institute of Medical Biology, Chinese Academy of Medical Sciences (DWSP202202004). All experimental operations were executed under anesthesia and abide by relevant ethical regulations.

2.2. Cells and viruses

Human embryonic kidney cell HEK293T, and African green monkey kidney cell Vero E6 were cultured in Dulbecco's modified Eagle's medium (DMEM; Gibco) supplemented with 10% Fetal

Bovine Serum (Gibco) and penicillin−streptomycin (1 ×) (M&C Gene Technology). Human cervical carcinoma cell HeLa with ACE2 overexpressing (Hela-ACE2) was maintained in DMEM with 10% FBS and 2 μg/mL puromycin (Yeasen).

SARS-CoV-2 strains were provided by Chinese or Guangdong Center for Disease Control and Prevention, Institute of Laboratory Animals Science, CAMS (Beijing, China). All infectious SARS-CoV-2 including prototype GD108 (GDPCC-nCOV27), Alpha (SARS-CoV-2/C-Tan-BJ202101(B1.1.7), CSTR.16698.06. NPRC 2.062100002), Beta (GDPCC-nCOV84, CSTR.16698.06. NPRC 2.062100001), Delta (CQ79, CSTR.16698.06. NPRC 6. CCPM-B-V-049-2105-8), Omicron BA.1 (CCPM-B-V-049-2112-18), and Omicron XBB.1.16 (isolated and kept by IMBCAMS) were passaged and performed under Biosafety Level 3 facilities in IMBCAMS. SARS-CoV-2 pseudovirus was purchased from Nanjing Vazyme Biotech Co., Ltd., including Prototype (DD1702-01/02/03), Delta (DD1754-01/02/03), Omicron BA.1 (DD1768-01/02/03), BA.2.12.1 (DD1777-01/02/03), BA.4/5 (DD1776-01/02/03).

2.3. Quality analysis of RG001 mRNA

The integrity and purity of RG001 mRNA were assessed by using the Agilent 5200 Fragment Analyzer Systems with the Agilent RNA Kit (15 nt) (Agilent) according to the manufacturer's instructions.

2.4. Electron microscopy of RG001

RG001 sample (2.5 μL) was deposited on a holey carbon grid that was glow-discharged (Quantifoil R1.2/1.3) and vitrificated using a Vitrobot Mark IV (Thermo Fisher Scientific) instrument. Cryo-TEM imaging was conducted on a Talos F200C Equipped with a Ceta 4 k × 4 k camera, operated at 200 kV accelerating voltage.

2.5. RG001 mRNA transfection

2×10^5 HEK293T cells/well were seeded in a 6-well plate. 1 μg RG001 candidates were respectively added into the supernatants of cells for 48 h incubation. Then cells were collected for S glycoprotein detection by western blotting as described below.

2.6. Western blotting

Transfected cells were harvested and lysed in buffer containing 25 mmol/L Tris, pH 7.4, 150 mmol/L NaCl, 1% NP-40, 1 mmol/L EDTA, and 5% glycerol (Pierce) on ice, and cell debris was removed by centrifugation at 12,000 rpm (Fresco 21, Thermo Fisher Scientific, MA, USA) for 10 min. Cellular extracts were subjected to SDS-PAGE and transferred onto 0.45 μm polyvinylidene difluoride (PVDF) membranes, further, incubated with SARS-CoV-2 S protein antibody (SinoBiological, 40591-T62), SARS-CoV-2 S2 antibody (Sino Biological, 40590-MM05) and horse radish peroxidase (HRP) conjugated secondary antibody. Blots were imaged with a ChemiDoc XRS + Imager (BIO-RAD) using the Image Lab software.

2.7. Mouse vaccination

6−8 weeks old female BALB/c mice were immunized intramuscularly with 5 μg RG001 candidates or placebo (empty LNPs) in a volume of 50 μL per mouse ($n = 5$) and boosted with an equivalent dose on Day 14 post-initial immunization. Sera were collected on Days 7, 14, 21, and 28 after initial immunization for detection of SARS-CoV-2-specific IgG and neutralizing antibody titers. Splenocytes were collected on Day 28 post-initial immunization for cellular immunity analysis by enzyme-linked immunospot (ELISpot) assay.

2.8. Rhesus macaque vaccination and virus challenge

Rhesus macaques were immunized intramuscularly with a low dose of 30 μg or a high dose of 100 μg RG001 Delta-S(P6) or PBS as placebo per macaque ($n = 4$, 2 male and 2 female macaques) and boosted with an equivalent dose on Day 21 post-initial immunization. Blood was collected on Days 0, 7, 14, 21, 27, and 35 after initial immunization for detection of SARS-CoV-2-specific IgG and neutralizing antibody titers. PBMCs were collected on Day 35 post-initial immunization for cellular immunity analysis by ELISpot assay. The host protection of RG001 in rhesus macaques was evaluated by challenging immunized rhesus macaques with 1×10^6 PFU of SARS-CoV-2 Delta (Indian strain) through both intranasal and intratracheal routes on Day 28 after booster immunization. The nasal, oropharyngeal, and anal swabs collection on Days 0, 1, 3, 5, and 7 post-infection (dpi) and lung anatomy were performed at 7 dpi under anesthesia for SARS-CoV-2 genomic RNA or subgenomic transcripts analysis and pulmonary histopathology assay. The macaque body weight and temperature changes were monitored and recorded at 0, 1, 3, 5, and 7 dpi.

2.9. ELISA for SARS-CoV-2 specific IgG antibody

SARS-CoV-2 S specific IgG antibody titers of sera collected from immunized mice or Rhesus macaques were determined by the commercial enzyme-linked immunosorbent assay (ELISA) kits (Sino Biological, KIT40588A, KIT40591A) according to the manufacturer's instructions. JN.1 S protein was purchased from Sino Biological (40589-V08H59) and coated into ELISA plates for JN.1 S-specific IgG analysis. Briefly, serial 5-fold dilutions of inactivated serum, starting at 1:100, were added to blocked 96-well plates (100 μL/well) coated with recombinant SARS CoV-2 S antigen, and plates were incubated for 2 h at room temperature. Meanwhile, add 100 μL SARS-CoV-2 S1 specific IgG antibody offered by the kits for positive control and 100 μL dilution buffer for negative control. After five washes with washing buffer (300 μL/well), plates were added with 1:100 diluted horseradish peroxidase (HRP)-conjugated rabbit anti-mouse IgG antibody or HRP-conjugated goat anti-human IgG antibody (100 μL/well) and incubated for 60 min at room temperature. Following five washes, the TMB substrate solution is loaded onto the plate (200 μL/well) for 20 min of incubation protecting it from light at room temperature. The color of samples develops in proportion to the amount of SARS-CoV-2 S1 specific IgG antibody. The reaction is stopped by the addition of a stop solution (50 μL/well) and the optical density at 450 nm (OD_{450}) of each well can be measured using a microplate reader (EnSpire). The cut-off value was defined according to the manufacturer's instructions. Eq. (1) can be used to calculate the endpoint antibody titer within the appropriate OD value range.

$$\text{Endpoint antibody titer} = \text{OD value of the sample well/Cut-off value} \times \text{Dilution} \quad (1)$$

2.10. Pseudovirus-based neutralization assay

2.10.1. Mice

The pseudovirus-based neutralization activity of immunized mouse serum was measured using a single-round pseudovirus to infect Hela-ACE2 cells. In brief, Hela-ACE2 cells were seeded in a 96-well plate at a concentration of 2×10^4 cells/well and cultured for approximately 24 h until about 90% confluence of cells. 2-fold serially diluted sera from immunized mice commencing with an initial dilution of 1:32 were incubated with an equal volume of the SARS-CoV-2 pseudotyped virus (1×10^4 $TCID_{50}$/mL) (Vazyme Biotech) for 1 h at 37 °C. Then the mixture was added to pre-seeded Hela-ACE2 cells for 48 h incubation. Cells were washed twice with PBS and lysed with Luciferase Cell Culture Lysis Reagent (Promega). The Luciferase activity in lysates was measured by using the Luciferase Assay System (Promega) with Centro LB960 Microplate Luminometer (Berthold Technologies). PNT_{50} was defined as the dilution of the serum at which the relative luminescence units (RLUs) of the cell lysates were reduced by 50% compared with those derived from cells infected with SARS-CoV-2 pseudoviruses in the absence of serum. The PNT_{50} was interpolated from the neutralization curves determined by 4-parameter nonlinear regression, *i.e.*, the log (inhibitor) *vs.* normalized response (variable slope), using GraphPad Prism 8.0. Each sample was tested three times.

2.10.2. Rhesus macaques

Pseudovirus-based neutralization activity of immunized rhesus macaque serum was measured by the same method as mice except with different strains of pseudotyped SARS-CoV-2.

2.11. SARS-CoV-2 neutralization assay

The immune sera collected from mice or Rhesus macaques were diluted in serial 2-fold dilutions from 1:16 to 1:2048 and then incubated with equal volumes of SARS-CoV-2 (100 $TCID_{50}$) respectively, including Prototype (GD108), Alpha, Beta, Delta, Omicron (BA.1, XBB.1.16). After 1 h of incubation at 37 °C, the mixture (100 μL/well) was added into the culture of Vero E6 cells seeded in a 96-well plate for 5 days of incubation. Meanwhile, cells were incubated only with mediums for negative control and with undiluted viruses for positive control. The cytopathic effect (CPE) of Vero E6 cells was observed and recorded under the microscope. Virus-neutralization titer (VNT_{50}) was defined as the highest dilution of the serum at which 50% CPE of cells was inhibited.

2.12. ELISpot assay

2.12.1. Mice

The antigen-specific cytokine-producing T cells derived from mouse splenocytes were assessed using interferon-γ (IFNγ) or interleukin-2 (IL-2) antibody precoated ELISpot assay kits (MabTech) to evaluate the cellular immune responses in the vaccinated mice, following the manufacturer's instruction. Briefly, the plates were washed 4 times with PBS ahead of being blocked with RPMI-1640 complete culture medium containing 10% FBS for at least 30 min at room temperature. The mouse splenocytes were dispersed in RPMI-1640 medium and then inoculated into the plate at the concentration of 100,000 cells/well. The SARS-CoV-2 S peptide pool (final concentration of 2.5 μg/mL) was added into the cell culture medium to stimulate antigen-specific cellular immune responses. After incubation at 37 °C, 5% CO_2 for 24 h, the plate was washed 5 times with PBS and then incubated with a biotinylated anti-mouse IFNγ or IL-2 detection antibody for 2 h at room temperature. After the same washes as above, the alkaline phosphatase labeled streptavidin (ALP-SA) was added to the plate for 1-h incubation at room temperature. Following the washing of the plate, the spots were developed with the addition of the ALP substrate solution. Count spots using the ImmunoSpot S6 Universal M2 Analyzer (CTL).

2.12.2. Rhesus macaques

PBMCs, isolated from rhesus macaque blood by centrifugation and lysis of red blood cells, were tested with nonhuman primate IFNγ or IL-2 ELISpot assay kits (MabTech). PBMCs were resuspended in RPMI-1640 complete culture medium and inoculated into the plate at the concentration of 1,000,000 cells/well. Full-length S of prototype, Delta, and Omicron (BA.1) peptide pools were used as stimuli with a final concentration of 2.5 μg/mL respectively to evaluate the cross-cellular immune responses elicited by RG001. The following steps are the same as above.

2.13. Analysis of genomic RNA and subgenomic transcripts of SARS-CoV-2 by RT-qPCR

Viral RNAs in both swab samples (nose, throat, and intestine) and lung lobes from SARS-CoV-2 challenged rhesus macaques were detected by quantitative reverse transcription PCR (RT-qPCR). Briefly, the total viral RNAs in homogenized samples were extracted using TRIzol LS reagent (Invitrogen) according to the manufacturer's protocol. SARS-CoV-2 genomic RNA quantification was performed by targeting the *N* gene of SARS-CoV-2 while viral subgenomic transcripts were quantified by targeting the *E* gene of SARS-CoV-2 using One Step TB Green PrimeScript RT-PCR Kit (Takara) with the specific primers: *N* gene forward primer: 5′-GACCCCAAAATCAGCGAAAT-3′; *N* gene reverse primer: 5′-TCTGGTTACTGCCAG TTGAATCTG-3′; *N* gene probe : 5′-FAM-ACCCCGCATTACGTTTGGTGGACC-BHQ1-3′. *E* gene forward primer: 5′-CGATCTCTTGTAGATCTGTTCTC-3′; *E* gene reverse primer: 5′-ATATTGCAGCAGTACGCACACA-3′; *E* gene probe : 5′-FAM-ACACTAGCCATCCTTACTGC GCTTCG-BHQ1-3′. Viral RNA load was expressed on a log10 scale as viral RNA equivalents per ml for swab samples and per g for lung tissue samples after comparison with a standard curve produced using serial 10-fold dilutions of SARS-CoV-2 RNA.

2.14. Hematoxylin and eosin (H&E) staining

For histopathology, different parts of the lungs from rhesus macaques were fixed in 4% neutral-buffered formaldehyde for 48 h, embedded in paraffin, and sectioned. Next, the fixed lung sections were subjected to hematoxylin and eosin (H&E) staining. Images were captured using the DHISTECH system equipped with a DP72 camera. Pulmonary pathological scores were measured according to the 6-grade scoring system.

2.15. Statistical analysis

Data are shown as mean ± standard deviations (SD) or mean ± standard error of mean (SEM). Statistical analysis was performed with two-way ANOVA and Multiple *t*-tests available in GraphPad Prism software. The significance of the difference is

indicated in the figures. *$P < 0.05$; **$P < 0.01$; ***$P < 0.001$; and n.s. denotes not significant.

3. Results

3.1. Design and expression of the RG001 mRNA vaccine against SARS-CoV-2

Due to the rapid emergence of SARS-CoV-2 VOCs, previous vaccines designed to target the S glycoprotein of the prototypical strain of SARS-CoV-2 have struggled to neutralize the new VOCs. Here we designed three RG001 candidates based on the full-length S protein of the Delta variant. In addition to the original Delta strain S protein as the immunogen (Delta-S), we developed two modified versions: Delta-S(P2), which includes substitutions of two residues (K984 and V985) to proline, and Delta-S(P6), which includes substitutions of six residues (F815, A890, A897, A940, K984, and V985) to proline. The latter two designs were expected to enhance the stability of pre-S conformation and increase the expression yield (Fig. 1A)[24]. Modified mRNAs were synthesized using *in vitro* transcription (IVT) and subsequently encapsulated within LNPs. Microfluidic capillary electrophoresis analyses of the encapsulated mRNAs revealed high integrity and purity across all three candidates (Fig. 1B). Cryo-transmission electron microscopy results showed that vaccine products exhibited homogeneous solid spheres, in contrast to the empty LNPs (Fig. 1C). To characterize the expression of RG001 candidate vaccines, we transfected HEK293T cells with each of the three candidates by directly introducing them to the culture medium. Robust expression of the cleaved forms of the S glycoprotein (Supporting Information Figs. S1 and S2) was observed for all candidates, with detected molecular weight of approximately 130 kDa and 100 kDa, respectively, as demonstrated by Western blot analysis (Fig. 1D).

3.2. Immunogenicity of RG001 mRNA vaccines in mice

We initially assessed the immunogenicity of RG001 candidates by immunizing BALB/c mice with a two-dose, two-week interval schedule. Mice were intramuscularly vaccinated with 5 μg mRNA per dose, using empty LNPs as the control. Sera were collected on Days 7, 14, 21, and 28 post-initial vaccination to evaluate the humoral immune response. Furthermore, mice spleens were harvested on Day 14 after the second dose of mRNA vaccination to measure the S-specific T cell immunity stimulated by the RG001 candidate vaccines (Fig. 2A). The first dose immunization by three RG001 candidates induced a steady increase in Delta-S specific serum IgG levels, as detected by ELISA, compared to inoculation with LNPs alone. Remarkably, during 7−14 days after the booster, the production of serum IgG surged dramatically, increasing more than 10-fold compared to the levels observed after the initial immunization. Geometric mean endpoint titers of serum IgG reached 159,154 (Delta-S), 164,385 (Delta-S(P2)) and 168,170 (Delta-S(P6)); however, there were no significant differences among three RG001 candidates (Fig. 2B). We performed a neutralization assay using HIV-based SARS-CoV-2 VOC pseudoviruses to measure the inhibition of virus entry by mouse antisera. As shown in Fig. 2C, sera from mice immunized with the Delta-S(P2) and Delta-S(P6) vaccines retained higher neutralizing activities against pseudovirus bearing the S glycoproteins of SARS-CoV-2 prototype (D614G) and Delta (B.1.617.2) than the Delta-S vaccine. Moreover, the 50% pseudovirus neutralization titer (PNT_{50}) induced by two doses of Delta-S(P6) against Omicron (BA.1) reached 992, ∼2−4 folds higher than the other two candidates (Fig. 2C). Further, the same serum samples were also applied for measurement of inhibitory effects on SARS-CoV-2 VOCs infection by using a CPE neutralization assay. Consistent with the results of pseudovirus neutralization, all three vaccine candidates induced robust neutralizing antibodies against the Prototype, Alpha, Beta, Delta, and Omicron variants. Importantly, serum from Delta-S(P6)-vaccinated mice showed strong inhibition on all types of SARS-CoV-2 infection with the highest 50% VNT_{50} geometric mean titers (GMT). Especially, the neutralization titer against Omicron was significantly higher than those induced by Delta-S and Delta-S(P2) (Fig. 2D).

We further characterized the S glycoprotein-specific response of splenic T cells after prime-booster vaccination with RG001 candidates by ELISpot assay. Total splenocytes collected on Day 28 after initial immunization were restimulated with the peptide pool of full-length Delta S protein and subjected to cytokine analysis. The patterns of T cell immune response induced by the three vaccine candidates were similar. ELISpot data revealed a ∼7-fold and ∼10-fold increase in IFNγ (Fig. 2E) and IL-2 (Fig. 2F) production of splenocytes, respectively, from all RG001-vaccinated mice compared with the control group. Overall, RG001 mRNA-LNP vaccine candidates demonstrated excellent potential to stimulate strong humoral and cellular immunity, and Delta-S(P6) appeared superior to the other two candidates in stimulating neutralizing antibodies.

3.3. RG001-elicited immunogenicity in rhesus macaques

Next, we assessed Delta-S(P6)-elicited immunogenicity in a non-human primate model. Groups of four rhesus macaques were intramuscularly injected with 30 or 100 μg of Delta-S(P6) or LNP control on Day 0 (prime) and Day 21 (booster) respectively (Fig. 3A). On Day 14, the S-specific IgG induced by Delta-S(P6) vaccination began to be detected. The IgG titers further increased 6 days after the booster (Day 27), then slightly decreased on Day 35. The IgG titers induced by either the low-dose group (30 μg) or the high-dose group (100 μg) remained at the same level (Fig. 3B). The same sera samples were also subjected to SARS-CoV-2 neutralization assay. On Day 14 after the first dose, the neutralizing antibodies against the prototype and Alpha, Beta, and Delta variants were detected in the sera of mice immunized with 30 or 100 μg Delta-S(P6). A strong boosting effect appeared on Day 6 after vaccination with the second dose. The highest level of neutralization GMT reached up to 3328 against prototype (100 μg), 1920 against alpha (100 μg), 496 against beta (30 μg), and 2048 against Delta (100 μg) on Day 35. Additionally, anti-Omicron neutralizing antibody was detected after booster immunization (Day 27), with GMTs continuing to rise by Day 35 (168 for 30 μg, 224 for 100 μg) (Fig. 3C−G). To further explore the neutralizing activity against more SARS-CoV-2 Omicron subvariants, a series of Omicron (BA.1, BA.2.12.1, BA.4/5 lineages) pseudovirus were used to quantify PNT_{50} of sera from RG001-immunized macaques by Day 14 after booster vaccination. Strong neutralizing effects against prototype and Delta pseudovirus were observed, consistent with data from the SARS-CoV-2 neutralization assay. Notably, the PNT_{50} against Omicron subvariants in rhesus macaques immunized with 30 and 100 μg of Delta-S(P6) reached ∼826 and ∼1172 for BA.1, ∼570 and ∼905 for BA.2.12.1, and ∼364 and ∼463 for BA.4/5,

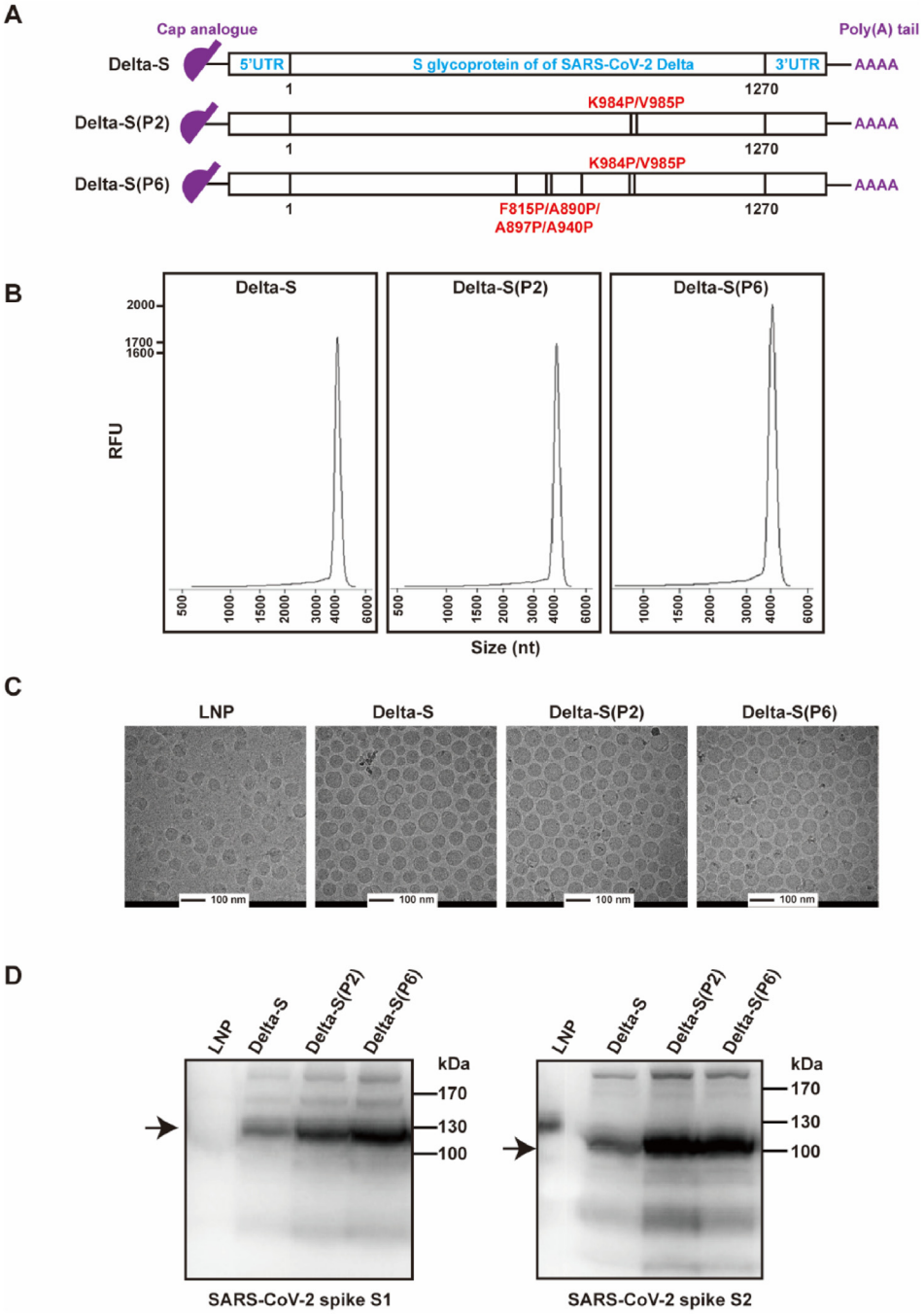

Figure 1 Design and expression of three RG001 SARS-CoV-2 mRNA vaccine candidates. (A) Schematic representation of three RG001 mRNA candidates engineered to express the full-length S protein of the SARS-CoV-2 Delta variant, along with S(P2) and S(P6) mutants. (B) Analysis of the integrity and purity of the three RG001 mRNA candidates using microfluidic capillary electrophoresis. (C) Cryo-transmission electron microscopy (Cryo-TEM) images showing both the empty LNPs and the three RG001 mRNA-LNPs; scale bar: 100 nm. (D) HEK293T cells were incubated with 1 μg of either RG001 mRNA-LNP or empty LNP for 48 h, followed by the detection of S1 and S2 glycoproteins *via* Western blot.

respectively, suggesting that Delta-S(P6) has the potential to induce broad-spectrum neutralizing antibody in macaques against various SARS-CoV-2 VOCs (Fig. 3H).

SARS-CoV-2-specific T cell immune response was strongly stimulated by two doses of Delta-S(P6) immunization. ELISpot results showed that either IFNγ or IL-2 in splenocytes from Delta-S(P6) vaccine-immunized macaques were highly stimulated by peptide pools of full-length S of prototype, Delta and Omicron (BA.1) compared with the control group. Both low and high-dose vaccine groups exhibited consistent cellular immunity towards the prototype, and Delta and Omicron variants (Fig. 3I and J). Together, our data demonstrated that RG001 candidate Delta-S(P6) successfully stimulated a broad T-cell immune response toward various SARS-CoV-2 VOCs.

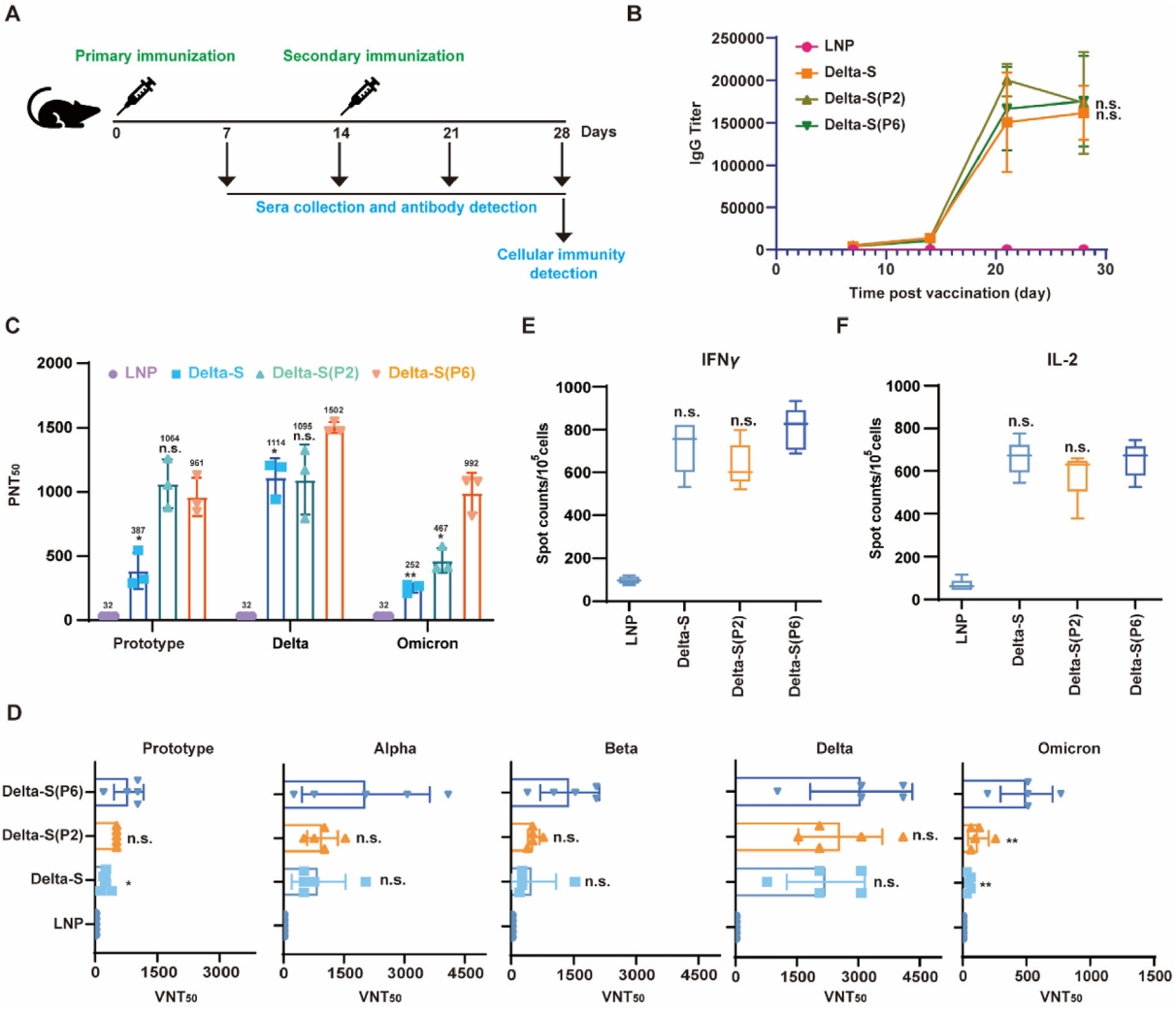

Figure 2 Humoral and cellular immune responses in RG001-vaccinated mice. (A) Schematic diagram of immunization (Days 0 and 14), serum collection (Days 7, 14, 21, and 28) for antibody detection, and splenocytes collection (Day 28) for cellular immunity analysis. Female BALB/c mice were injected *via* i.m. with 5 μg RG001 candidates or empty LNPs per mouse ($n = 5$) and boosted with an equivalent dose. (B) The Delta-specific IgG antibody titer was quantified by ELISA. Values are shown as mean ± SD, two-way ANOVA analysis was used to calculate *P* values relative to a group of Delta-S(P6) (n.s., not significant). (C) Detection of 50 % pseudovirus (Prototype (D614G), Delta (B.1.617.2) and Omicron (BA.1)) neutralization titer (PNT_{50}) of sera from RG001-immunized mice. Sera from the five mice of the same group were mixed as one sample and analyzed three times. (D) Measurement of SARS-CoV-2 virus (Prototype (GD108), Alpha, Beta, Delta and Omicron (BA.1)) VNT_{50} of sera from RG001-immunized mice. (E) ELISpot assay for IFNγ in mice splenocytes. (F) ELISpot assay for IL-2 in mice splenocytes. (C–F) Every bar represents mean ± SD ($n = 5$). Multiple *t*-test were used to calculate *P* values relative to a group of Delta-S(P6) (n.s., not significant; $^{*}P < 0.05$; $^{**}P < 0.01$).

3.4. *RG001-elicited viral suppression in rhesus macaques*

Host protection by RG001 in Rhesus macaques was evaluated by challenging 1×10^6 $TCID_{50}$/mL of SARS-CoV-2 Delta (Indian strain) through both intranasal and intratracheal routes on Day 28 after booster immunization. We collected nasal, oropharyngeal, and anal swab samples under anesthetic conditions for viral load measurement at 1, 3, 5, and 7 dpi, and eventually lung tissue samples from sacrificial macaques were harvested for SARS-CoV-2 genomic RNA and subgenomic transcript analysis.

Due to the robust neutralizing antibody, SARS-CoV-2 genomic RNA (SARS-CoV-2 *N* gene) in nasal, oropharyngeal, and anal samples from Delta-S(P6)-immunized macaques dramatically decreased compared with the LNP control group. From Day 1 to Day 7 after the virus challenge, viral loads in all samples from empty LNPs-vaccinated macaques were maintained at high levels with slight fluctuations. In contrast, Rhesus macaques injected with 30 or 100 μg RG001 showed $\sim 10^{3.52}$- or $\sim 10^{2.02}$-fold reduction in the nose (Fig. 4A), $\sim 10^{2.94}$- or $\sim 10^{2.68}$-fold reduction in the throat (Fig. 4B), and $\sim 10^{1.43}$- or $\sim 10^{3.02}$-fold decrease in the intestine at 7 dpi (Fig. 4C), respectively, suggesting strong virus-clearance by RG001 vaccination. Furthermore, viral genomic RNA in lung fragments was dramatically decreased by RG001 immunization with dose-dependent effects (Low dose: $\sim 10^{0.65}$–$10^{2.19}$-fold reduction, High dose: $\sim 10^{1.71}$–$10^{5.34}$-fold reduction), indicating that high dose RG001

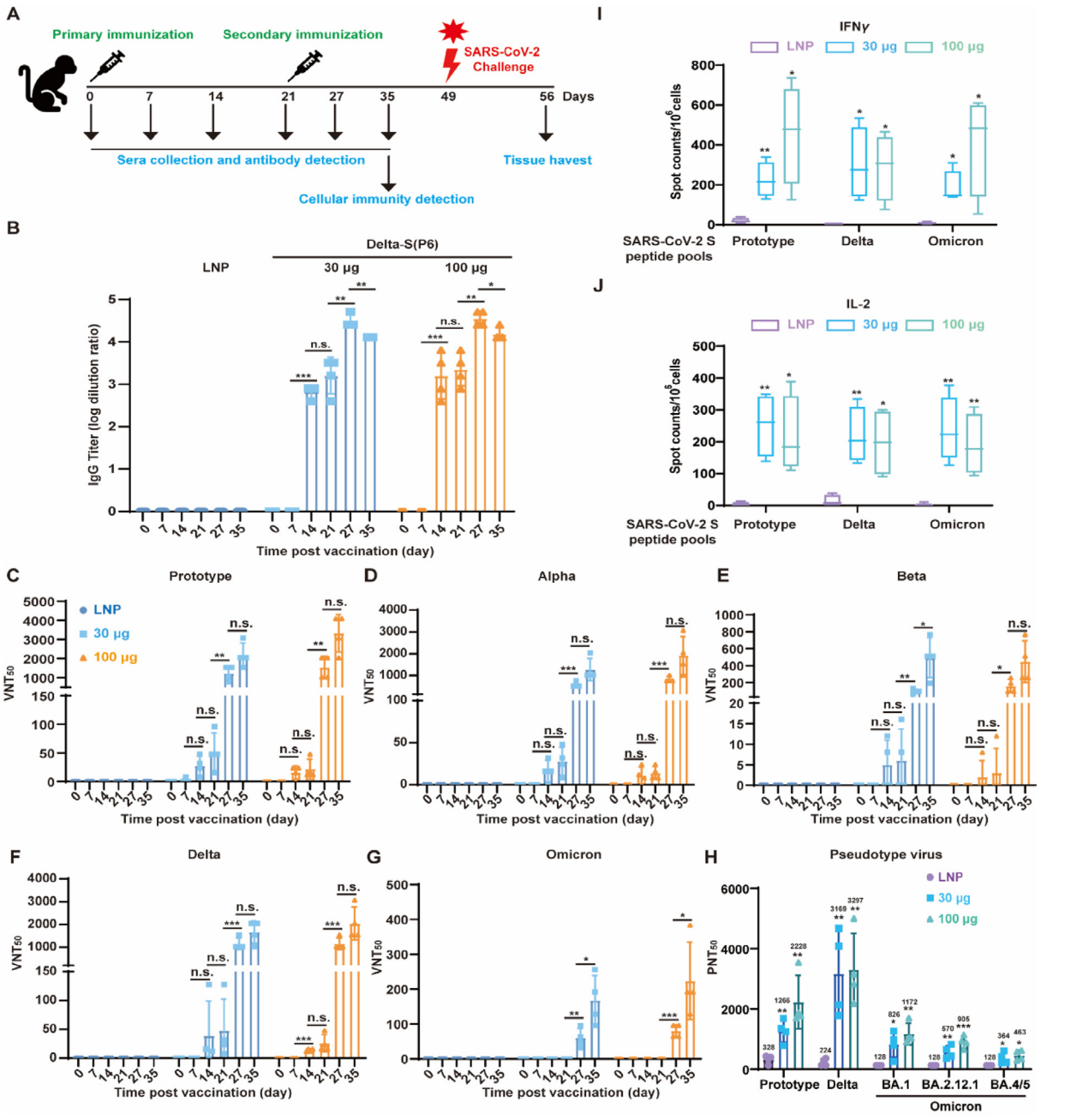

Figure 3 Humoral and cellular immune responses in RG001-vaccinated Rhesus macaques. (A) Schematic diagram of immunization (Days 0 and 21), serum collection (Days 0, 7, 14, 21, 27, and 35) for antibody detection, PBMCs collection (Day 35) for cellular immunity analysis, virus challenge for immuno-protection (Day 49). Rhesus macaques were immunized *via* i.m. with 30 μg or 100 μg of RG001 Delta-S(P6) or PBS per macaques ($n = 4$) and boosted with an equivalent dose. (B) Delta-specific IgG antibody titer was quantified by ELISA. (C−G) SARS-CoV-2 neutralizing assay for VNT_{50} against the prototype (GD108) and Alpha, Beta, Delta, and Omicron (BA.1) variants. (B−J) Every bar represents mean ± SD ($n = 4$). Multiple *t*-test were used to calculate *P* values (n.s., not significant; $^{*}P < 0.05$; $^{**}P < 0.01$; $^{***}P < 0.001$). (H) Pseudovirus neutralizing assay for PNT_{50} against prototype, Delta, and Omicron (BA.1, BA.2.12.1, and BA.4/5). (I) ELISpot assay for IFNγ in macaques PBMCs. (J) ELISpot assay for IL-2 in macaques PBMCs. (H−J) Every bar represents mean ± SD ($n = 4$). Multiple *t*-test were used to calculate *P* values relative to the group of LNP (n.s., not significant; $^{*}P < 0.05$; $^{**}P < 0.01$; $^{***}P < 0.001$).

vaccination displayed a stronger effect on pulmonary viral elimination than low dose. Besides, viral subgenomic transcript (SARS-CoV-2 *E* gene) was virtually undetectable in any parts of dissected lung tissues from macaques vaccinated with either dose of RG001, suggesting a strong inhibition of SARS-CoV-2 replication (Fig. 4D).

3.5. *RG001-elicited tissue protection in rhesus macaques*

The RG001 vaccine significantly contributed to strong tissue protection by reducing SARS-CoV-2 infection. All samples of lung sections were applied for H&E staining and pathological analysis. Macaques vaccinated with LNPs developed obvious lung

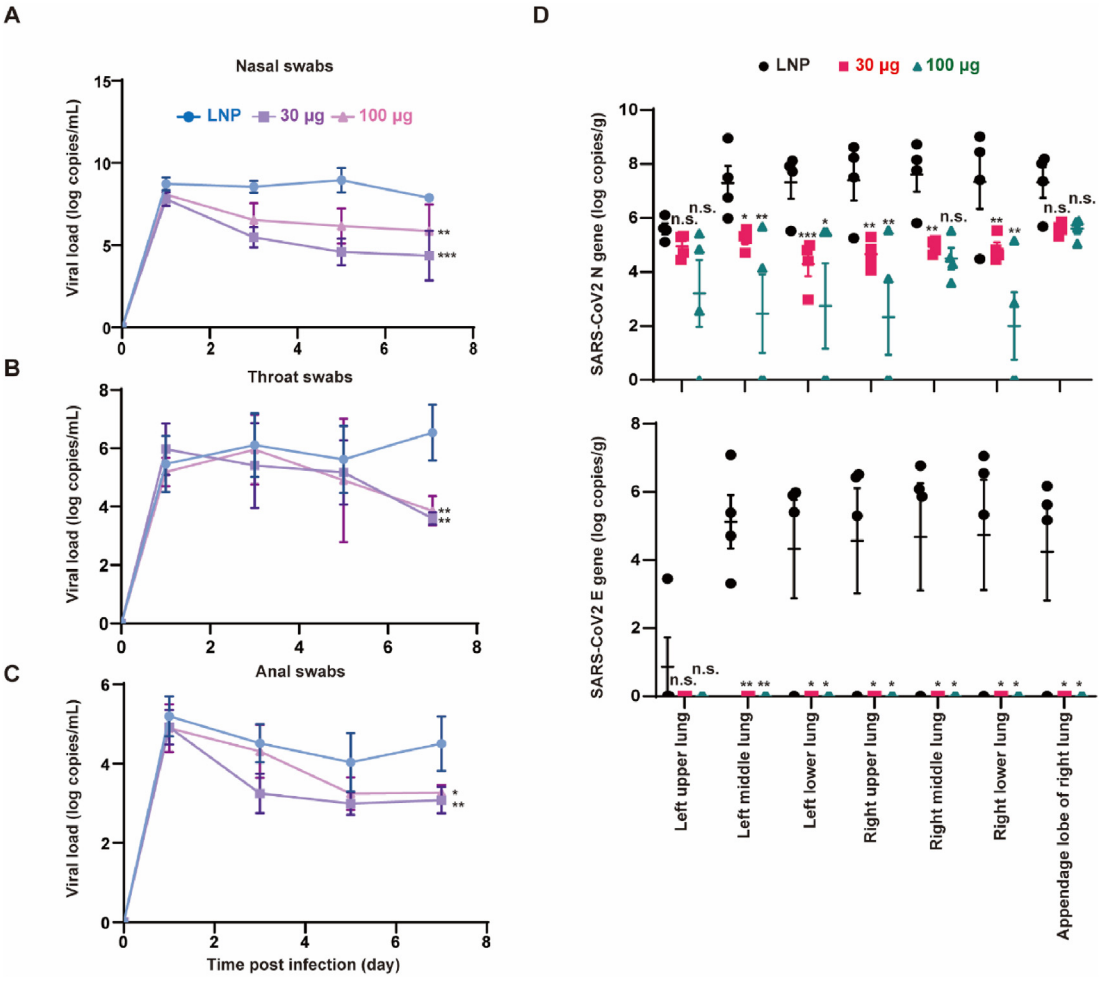

Figure 4 Effects of RG001 in viral clearance. SARS-CoV-2 genomic RNA (SARS-CoV-2 *N* gene) in (A) nasal swab, (B) throat swab, and (C) anal swab samples collected from rhesus macaques respectively immunized with LNPs, 30 μg or 100 μg RG001 were detected by RT-qPCR. Data are shown as mean ± SD ($n = 4$). (D) SARS-CoV-2 genomic RNA and subgenomic transcripts in lung tissues were measured by RT-qPCR. Values are shown as mean ± SEM ($n = 4$). Two-way ANOVA was used to calculate *P* values relative to the group of LNP (n.s., not significant; $^{*}P < 0.05$; $^{**}P < 0.01$; $^{***}P < 0.001$).

lesions, characterized by thickened alveolar septa accompanied by congestion, exudation, and infiltration of mainly inflammatory lymphocytes and macrophages in the alveolar interstitium. The formation of vascular thrombus and slight anthracosis were also observed. For comparison, lung sections from macaques immunized with Delta-S(P6) only developed slight congestion and infiltration of inflammatory cells in the alveolar interstitium with a lower pathological score than the control group (Fig. 5 and Fig. S1). Moreover, both body weight and temperature of vaccinated macaques were maintained in normal ranges (Fig. S2), suggesting a high degree of tissue protection by RG001 vaccination.

3.6. RG001 elicited protection against emerging Omicron subvariants

The emergence of SARS-CoV-2 Omicron variant BA.2 sublineages XBB and JN.1 caused a high level of escape from established immunity by previous vaccines, and currently, its descendants dominate globally. To further evaluate the immunogenicity of RG001-Delta-S(P6) against emerging Omicron subvariants, we applied the third dose of the vaccine in Rhesus macaques and mice. Mouse sera were collected on Days 7, 14, 21, 28, 35, and 42 post-initial vaccination, respectively, for Delta, BA.1, and JN.1 S-specific IgG titer evaluation. Animal sera collected on Day 14 post the second and third vaccinations were analyzed for neutralizing antibodies against Delta, BA.1, XBB.1.16, and JN.1 (Fig. 6A). The third immunization elevated neutralization GMTs of Rhesus macaque sera compared with the secondary booster (Delta: ∼1.3-fold, BA.1: ∼1.8-fold). Moreover, the neutralizing antibody against XBB.1.16 was successfully induced by the third booster (XBB.1.16 GMTs: 85) (Fig. 6B). A three-dose vaccination regimen with RG001 also progressively elevated serum IgG levels specific to Delta, BA.1, and JN.1 S in immunized mice. By Day 42, the IgG levels for JN.1 S were ∼6.88- and ∼3.66-fold lower than those for Delta and BA.1, respectively (Fig. 6E). PNT_{50} elicited by the third dose of RG001 against the JN.1 variant reached 154, which was ∼3 folds higher than that achieved by the second booster. Although the neutralization GMTs against JN.1 was significantly lower than those for

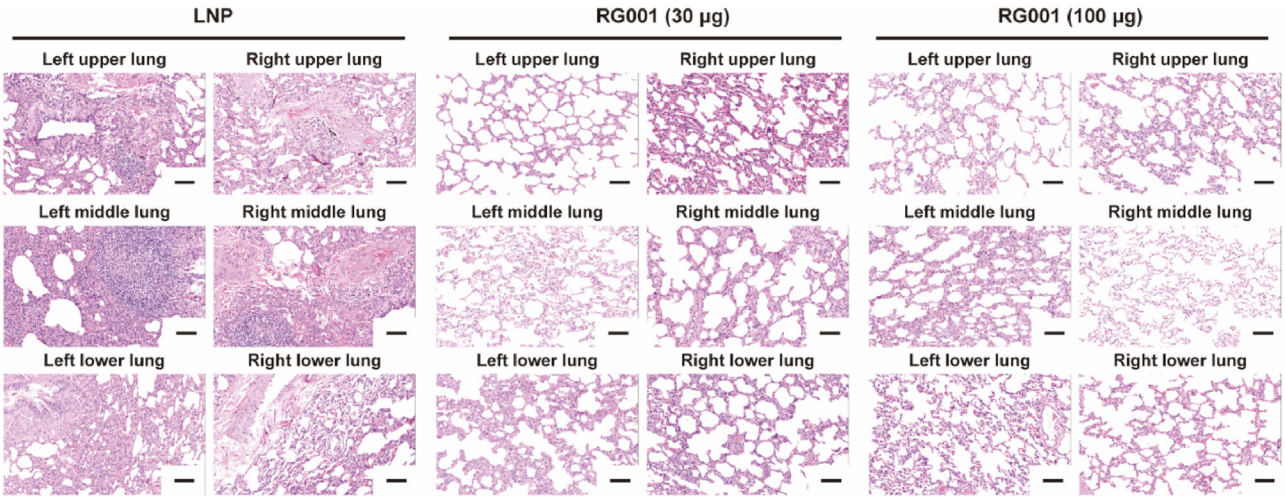

Figure 5 Pulmonary protection in rhesus macaques by RG001 vaccination. H&E staining of lung fragments pathology. Representative images from 4 rhesus macaques are shown. Scale bar, 100 μm.

Delta, the neutralizing capacity remained effective and detectable (Fig. 6F). This indicates that additional sequential boosters of RG001 could potentially enhance the production of neutralizing antibodies against emerging SARS-CoV-2 VOCs.

While humoral immunity is crucial for the protection from SARS-CoV-2 infection, cellular immunity stimulated by vaccines plays an important function in long-term cross-protection. To assess the T cell immune response against XBB variant, mice were immunized with two doses of RG001. Subsequently, splenocytes were collected and stimulated by Delta, BA.1, XBB.1, and JN.1 S peptide pools on Day 28 post immunization, respectively (Fig. 6A). Surprisingly, T-cell responses displayed a different trend compared with neutralizing antibody levels. Specifically, cellular immune responses against BA.1 and XBB.1 were maintained at similar levels for both IFNγ and IL-2. However, they were almost significantly higher than those against the Delta variant (IFNγ: BA.1, ∼2.99-fold, $P < 0.001$; XBB.1, ∼3.58-fold, $P < 0.001$; IL-2: BA.1, ∼1.47-fold, $P < 0.01$) (Fig. 6C and D). Simultaneously, IFNγ and IL-2 positive lymphocytes in mouse spleens induced by either JN.1 or BA.1 S peptide pools kept consistent (Fig. 6G and H). Taken together, even RG001 immunization elicited relatively lower neutralizing antibody levels against Omicron XBB and JN.1 compared with Delta, higher T cell response induced by prime-boost vaccination might successfully ensure the vaccine efficiency to prevent current epidemic SARS-CoV-2 variants infection.

4. Discussion

As the emergence of Omicron variants, especially BA.2.75, XBB, and JN.1 derived from BA.2 exhibited a strong immune evasion, which caused the collapse of the immune defense system constructed by vaccines and outbreaks of new pandemic waves[25]. New vaccines against emerging SARS-CoV-2 VOCs and vaccination strategies were emergently called for. In this study, we developed a mRNA-LNP vaccine based on Delta S glycoprotein distinguished with approved mRNA vaccines, which exhibited a strong immunogenicity in the production of neutralizing antibodies and activation of SARS-CoV-2 VOCs-specific T cell responses, especially for Omicron subvariant XBB, which represented a comprehensive immune response to counter SARS-CoV-2 intrusion and viral clearance.

RG001 mRNA vaccine candidate, Delta-S(P6), rapidly induced robust high neutralizing antibodies in either mouse or Rhesus macaque model with the inhibition of pseudovirus entry was comparable with neutralization elicited by wild-type monovalent mRNA vaccines[26,27]. Broad-neutralizing effects against various authentic SARS-CoV-2 including prototype, Alpha, Beta, Delta, and Omicron variants were also elicited by RG001 and the two approved mRNA vaccines, and neutralizing antibodies against Omicron strains induced by all vaccines showed more or less reductions compared with ancient strains, which agrees with results from clinical studies of human serum samples[28-30]. Especially, two-dose immunization of 100 μg RG001-induced neutralizing antibody GMTs against pseudovirus could reach 1172 for BA.1, 905 for BA.2.12.1, 463 for BA.4/5, moreover, nAb GMTs against BA.1 live-virus approached 235 in Rhesus macaques. Three-dose booster further elevated neutralizing effects with GMTs of 427 for BA.1 and 85 for XBB.1.16. The neutralizing activity against JN.1 with GMTs of 154 was also induced by triple-RG001 vaccination in a mouse model, which was similar to the neutralization of a wild-type monovalent vaccine combined with a bivalent booster[18,31]. Little data about nAbs for XBB and JN.1 induced by approved vaccines in non-human primate models have been reported; four of the approved monovalent mRNA vaccines failed to stimulate effective nAbs in human serum samples to counter XBB infection, but bivalent mRNA vaccine as a fifth dose was able to elicit a neutralization against circulating Omicron substrains[16,32,33]. Moreover, a recent study indicated that the original COVID-19 priming regimen reduced the immunogenicity of bivalent BA.1 or BA.5 boosters, and WHO recommended monovalent vaccines based on circulating strains[34]. Besides, the Delta−Omicron RBD mRNA vaccine induced higher neutralizing antibody titer against Omicron pseudovirus than the Omicron−Omicron RBD mRNA vaccine, suggesting the superiority of Delta immunogen in protection from Omicron sub-lineage variants infection[35]. The successful stimulation of multiple SARS-CoV-2 VOC-specific neutralizing antibodies by monovalent RG001 strongly enhanced the possibility of building a broad and fundamental immunity for protection against emerged and emerging SARS-CoV-2 sub-variants infection.

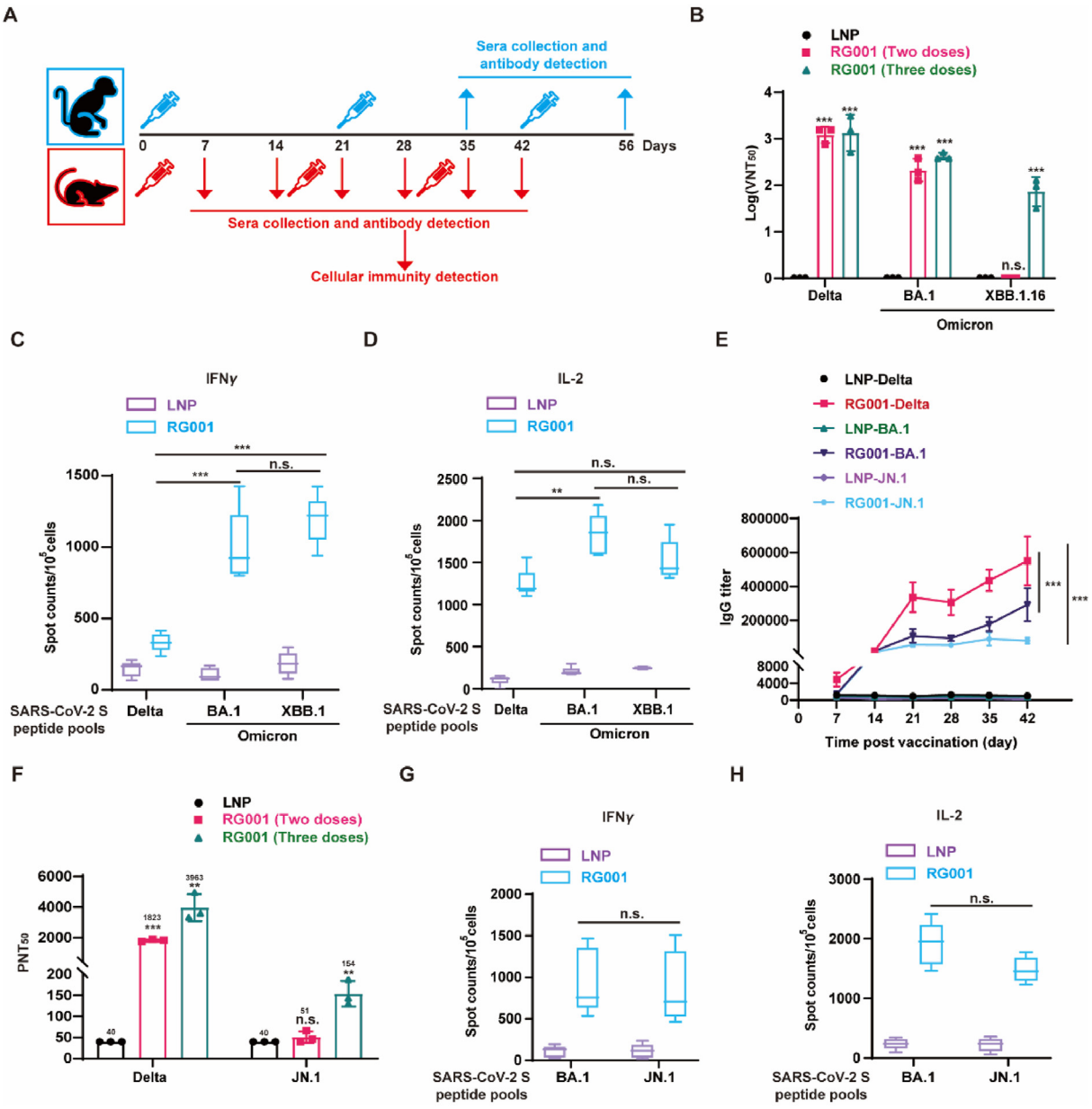

Figure 6 The protective effects of RG001 against emgerging Omicron subvariants. (A) Schematic diagram of (blue) rhesus macaque immunization (Days 0, 21, and 42), serum collection (Days 35 and 56) for neutralizing antibody detection, and (Red) mice vaccination (Days 0, 14, and 28) and splenocytes collection (Day 28) for cellular immunity analysis. (B) SARS-CoV-2 neutralizing assay for VNT_{50} against Delta and Omicron (BA.1, XBB.1.16) in sera from RG001-immunized Rhesus macaques. Data are shown as mean ± SD ($n = 3$). (C, G) ELISpot assay for IFNγ in mice splenocytes. (D, H) ELISpot assay for IL-2 in mice splenocytes. (E) Delta, Omicron (BA.1, JN.1)-specific IgG antibody titer was quantified by ELISA. Data are shown as mean ± SD ($n = 5$) (F) Pseudovirus neutralizing assay for 50 against Delta and Omicron (JN.1). Sera from the five mice of the same group were mixed as one sample and analyzed three times. Data are shown as mean ± SD. Two-way ANOVA (E) was used to calculate P values relative to group of Delta ($^{***}P < 0.001$), and Multiple t test was used to calculate P values (B, C, D, F, G, H) (n.s., not significant; $^{**}P < 0.01$; $^{***}P < 0.001$).

Besides humoral response, RG001 displayed similar strength to mRNA-1273 and BNT162b2 in the stimulation of a significant cellular immunity against all SARS-CoV-2 VOCs in both mice and Rhesus macaques[36,37]. Interestingly, two doses of RG001 immunization exhibited more effective T cell responses against Omicron (BA.1, XBB.1, JN.1) than Delta in mice, which probably make up the deficiency of nAbs production against XBB and JN.1, suggesting powerful cross-protection against emerging SARS-CoV-2 VOCs.

5. Conclusions

RG001 dramatically protected rhesus macaques from infection of pathogenic SARS-CoV-2 Delta strain and reduced viral loads. Particularly, undetectable subgenomic RNA in the lungs and rare clinical signs of disease and lesions in the lungs indicated strong virus defense and clearance by RG001 vaccination. Moderate pathological symptoms likely reflected interstitial pneumonia protection by RG001[38]. The effects of robust SARS-CoV-2 eradication

and body protection mediated by RG001 were consistent with the reported efficacy of mRNA vaccines[39]. Together, our preclinical data demonstrated the potency of RG001 as a potential mRNA vaccine candidate against multiple SARS-CoV-2 VOCs.

Acknowledgments

We thank Division for Medicinal Microorganisms Related Strains, CAMS Collection Center of Pathogenic Microorganisms (Beijing 100050, China) for providing valuable reagents. Hua Chen, Wei Qin, Shanshan Cao, Guanglong Liu, Yi Wang, Tianming Qi, Tingting Zhang and other colleagues at RinuaGene Biotechnology Co., Ltd. for mRNA sequence optimization, IVT, mRNA purification, and LNP formulation. This work was supported by Beijing Natural Science Foundation (7242097, China), CAMS Innovation Fund for Medical Sciences (2021-I2M-1−038, 2022-I2M-2-002, 2021-I2M-1−043, 2021-I2M-1−030, China).

Author contributions

Dongrong Yi: Writing − review & editing, Writing − original draft, Methodology, Investigation, Funding acquisition, Formal analysis, Data curation. Yongxin Zhang: Investigation, Formal analysis, Data curation. Jing Wang: Formal analysis, Data curation. Qian Liu: Investigation, Formal analysis, Data curation. Ling Ma: Investigation, Formal analysis, Data curation. Quanjie Li: Software, Investigation, Funding acquisition, Formal analysis. Saisai Guo: Visualization, Validation, Formal analysis. Ruifang Zheng: Formal analysis. Xiaoyu Li: Supervision, Funding acquisition. Xingong Li: Supervision, Project administration. Yijie Dong: Supervision, Project administration, Conceptualization. Shuaiyao Lu: Methodology, Investigation, Formal analysis, Data curation. Weiguo Zhang: Writing − review & editing, Supervision, Conceptualization. Xiaozhong Peng: Supervision, Resources, Conceptualization. Shan Cen: Writing − review & editing, Supervision, Project administration, Funding acquisition, Conceptualization.

Conflicts of interest

Shan Cen, Dongrong Yi, Jing Wang, and Yijie Dong are co-inventors on pending patent applications related to the SARS-CoV-2 mRNA vaccine. Xingong Li, Yijie Dong and Weiguo Zhang are employees of RinuaGene Biotechnology Co., Ltd.

Appendix A. Supporting information

Supporting information to this article can be found online at https://doi.org/10.1016/j.apsb.2024.12.003.

References

1. Carvalho T, Krammer F, Iwasaki A. The first 12 months of COVID-19: a timeline of immunological insights. *Nat Rev Immunol* 2021;**21**:245−56.
2. Kurhade C, Zou J, Xia H, Liu M, Yang Q, Cutler M, et al. Neutralization of Omicron sublineages and Deltacron SARS-CoV-2 by three doses of BNT162b2 vaccine or BA.1 infection. *Emerg Microbes Infect* 2022;**11**:1828−32.
3. Cao Y, Yisimayi A, Jian F, Song W, Xiao T, Wang L, et al. BA.2.12.1, BA.4 and BA.5 escape antibodies elicited by Omicron infection. *Nature* 2022;**608**:593−602.
4. Callaway E. What Omicron's BA.4 and BA.5 variants mean for the pandemic. *Nature* 2022;**606**:848−9.
5. Tegally H, Moir M, Everatt J, Giovanetti M, Scheepers C, Wilkinson E, et al. Emergence of SARS-CoV-2 omicron lineages BA.4 and BA.5 in South Africa. *Nat Med* 2022;**28**:1785−90.
6. Xia S, Wang L, Zhu Y, Lu L, Jiang S. Origin, virological features, immune evasion and intervention of SARS-CoV-2 Omicron sublineages. *Signal Transduct Target Ther* 2022;**7**:241.
7. Verbeke R, Hogan MJ, Loré K, Pardi N. Innate immune mechanisms of mRNA vaccines. *Immunity* 2022;**55**:1993−2005.
8. Skowronski DM, De Serres G. Safety and efficacy of the BNT162b2 mRNA covid-19 vaccine. *N Engl J Med* 2021;**384**:1576−7.
9. Li C, Lee A, Grigoryan L, Arunachalam PS, Scott MKD, Trisal M, et al. Mechanisms of innate and adaptive immunity to the Pfizer-BioNTech BNT162b2 vaccine. *Nat Immunol* 2022;**23**:543−55.
10. Liu Y, Liu J, Xia H, Zhang X, Fontes-Garfias CR, Swanson KA, et al. Neutralizing activity of BNT162b2-elicited serum. *N Engl J Med* 2021;**384**:1466−8.
11. Liu Y, Liu J, Xia H, Zhang X, Zou J, Fontes-Garfias CR, et al. BNT162b2-elicited neutralization against new SARS-CoV-2 spike variants. *N Engl J Med* 2021;**385**:472−4.
12. Regev-Yochay G, Gonen T, Gilboa M, Mandelboim M, Indenbaum V, Amit S, et al. Efficacy of a fourth dose of Covid-19 mRNA vaccine against Omicron. *N Engl J Med* 2022;**386**:1377−80.
13. Xia H, Zou J, Kurhade C, Cai H, Yang Q, Cutler M, et al. Neutralization and durability of 2 or 3 doses of the BNT162b2 vaccine against Omicron SARS-CoV-2. *Cell Host Microbe* 2022;**30**:485−8.e3.
14. Muecksch F, Wang Z, Cho A, Gaebler C, Ben Tanfous T, DaSilva J, et al. Increased memory B cell potency and breadth after a SARS-CoV-2 mRNA boost. *Nature* 2022;**607**:128−34.
15. Wang Q, Iketani S, Li Z, Liu L, Guo Y, Huang Y, et al. Alarming antibody evasion properties of rising SARS-CoV-2 BQ and XBB subvariants. *Cell* 2023;**186**:279−86.e8.
16. Zhang X, Chen LL, Ip JD, Chan WM, Hung IF, Yuen KY, et al. Omicron sublineage recombinant XBB evades neutralising antibodies in recipients of BNT162b2 or CoronaVac vaccines. *Lancet Microbe* 2023;**4**:e131.
17. Kurhade C, Zou J, Xia H, Liu M, Chang HC, Ren P, et al. Low neutralization of SARS-CoV-2 Omicron BA.2.75.2, BQ.1.1 and XBB.1 by parental mRNA vaccine or a BA.5 bivalent booster. *Nat Med* 2023;**29**:344−7.
18. Favresse J, Gillot C, Cabo J, David C, Dogné JM, Douxfils J. Neutralizing antibody response to XBB.1.5, BA.2.86, FL.1.5.1, and JN.1 six months after the BNT162b2 bivalent booster. *Int J Infect Dis* 2024;**143**:107028.
19. Ying B, Scheaffer SM, Whitener B, Liang CY, Dmytrenko O, Mackin S, et al. Boosting with variant-matched or historical mRNA vaccines protects against Omicron infection in mice. *Cell* 2022;**185**:1572−87.e11.
20. Wang Q, Guo Y, Bowen A, Mellis IA, Valdez R, Gherasim C, et al. XBB.1.5 monovalent mRNA vaccine booster elicits robust neutralizing antibodies against XBB subvariants and JN.1. *Cell Host Microbe* 2024;**32**:315−21.e3.
21. Kumari M, Su SC, Liang KH, Lin HT, Lu YF, Chen KC, et al. Bivalent mRNA vaccine effectiveness against SARS-CoV-2 variants of concern. *J Biomed Sci* 2023;**30**:46.
22. Qu L, Yi Z, Shen Y, Lin L, Chen F, Xu Y, et al. Circular RNA vaccines against SARS-CoV-2 and emerging variants. *Cell* 2022;**185**:1728−44.e16.
23. Qin S, Huang H, Xiao W, Chen K, He X, Tang X, et al. A novel heterologous receptor-binding domain dodecamer universal mRNA vaccine against SARS-CoV-2 variants. *Acta Pharm Sin B* 2023;**13**:4291−304.
24. Hsieh CL, Goldsmith JA, Schaub JM, DiVenere AM, Kuo HC, Javanmardi K, et al. Structure-based design of prefusion-stabilized SARS-CoV-2 spikes. *Science* 2020;**369**:1501−5.

25. Faraone JN, Qu P, Evans JP, Zheng YM, Carlin C, Anghelina M, et al. Neutralization escape of Omicron XBB, BR.2, and BA.2.3.20 subvariants. *Cell Rep Med* 2023;**4**:101049.
26. Vogel AB, Kanevsky I, Che Y, Swanson KA, Muik A, Vormehr M, et al. BNT162b vaccines protect rhesus macaques from SARS-CoV-2. *Nature* 2021;**592**:283−9.
27. Corbett KS, Edwards DK, Leist SR, Abiona OM, Boyoglu-Barnum S, Gillespie RA, et al. SARS-CoV-2 mRNA vaccine design enabled by prototype pathogen preparedness. *Nature* 2020;**586**:567−71.
28. Qu P, Faraone JN, Evans JP, Zheng YM, Yu L, Ma Q, et al. Durability of booster mRNA vaccine against SARS-CoV-2 BA.2.12.1, BA.4, and BA.5 subvariants. *N Engl J Med* 2022;**387**:1329−31.
29. Cameroni E, Bowen JE, Rosen LE, Saliba C, Zepeda SK, Culap K, et al. Broadly neutralizing antibodies overcome SARS-CoV-2 Omicron antigenic shift. *Nature* 2022;**602**:664−70.
30. Cao Y, Wang J, Jian F, Xiao T, Song W, Yisimayi A, et al. Omicron escapes the majority of existing SARS-CoV-2 neutralizing antibodies. *Nature* 2022;**602**:657−63.
31. Routhu NK, Stampfer SD, Lai L, Akhtar A, Tong X, Yuan D, et al. Efficacy of mRNA-1273 and Novavax ancestral or BA.1 spike booster vaccines against SARS-CoV-2 BA.5 infection in non-human primates. *Sci Immunol* 2023:eadg7015.
32. Solera JT, Ierullo M, Arbol BG, Mavandadnejad F, Kurtesi A, Qi F, et al. Bivalent COVID-19 mRNA vaccine against omicron subvariants in immunocompromised patients. *Lancet Infect Dis* 2023;**23**:e266−7.
33. Uraki R, Ito M, Kiso M, Yamayoshi S, Iwatsuki-Horimoto K, Furusawa Y, et al. Antiviral and bivalent vaccine efficacy against an omicron XBB.1.5 isolate. *Lancet Infect Dis* 2023;**23**:402−3.
34. Zaeck LM, Tan NH, Rietdijk WJR, Geers D, Sablerolles RSG, Bogers S, et al. Original COVID-19 priming regimen impacts the immunogenicity of bivalent BA.1 and BA.5 boosters. *Nat Commun* 2024;**15**:4224.
35. Han Y, An Y, Chen Q, Xu K, Liu X, Xu S, et al. mRNA vaccines expressing homo-prototype/Omicron and hetero-chimeric RBD-dimers against SARS-CoV-2. *Cell Res* 2022;**32**:1022−5.
36. Jung MK, Jeong SD, Noh JY, Kim DU, Jung S, Song JY, et al. BNT162b2-induced memory T cells respond to the Omicron variant with preserved polyfunctionality. *Nat Microbiol* 2022;**7**:909−17.
37. Sahin U, Muik A, Derhovanessian E, Vogler I, Kranz LM, Vormehr M, et al. COVID-19 vaccine BNT162b1 elicits human antibody and T_H1 T cell responses. *Nature* 2020;**586**:594−9.
38. Bao L, Deng W, Huang B, Gao H, Liu J, Ren L, et al. The pathogenicity of SARS-CoV-2 in hACE2 transgenic mice. *Nature* 2020;**583**:830−3.
39. Zhang NN, Li XF, Deng YQ, Zhao H, Huang YJ, Yang G, et al. A thermostable mRNA vaccine against COVID-19. *Cell* 2020;**182**:1271−83.e16.